Eur. Phys. J. D (2023) 77:61
https://doi.org/10.1140/epjd/s10053-023-00641-5

THE EUROPEAN PHYSICAL JOURNAL D

Regular Article – Atomic and Molecular Collisions

Universal axial rainbow channeling interaction potential

N. Starčević[a] and S. Petrović

Laboratory of Physics, Vinča Institute of Nuclear Sciences, University of Belgrade, P.O. Box 522, Belgrade, Serbia

Received 30 December 2022 / Accepted 21 March 2023 / Published online 13 April 2023

Abstract. This study is devoted to the construction of the universal ion–crystal interaction potential in proton transmission through very thin crystals. We show how to obtain the interaction potential by using the crystal rainbow theory and rainbows' morphological analysis in the proton transmission angular plane. By adjusting the shapes of rainbow lines, we modified the Molière's interaction potential to make it accurate in all regions of the crystal channels. This procedure was based on our previous experimental and theoretical works. As a result, the two axial channeling directions can be treated in the same way leading to more consistent values of the fitting parameters in the ion–atom interaction potential. We obtained the universal rainbow ion–crystal interaction potential for very thin cubic crystals in the (001) and (111) orientations in the case of transmission channeling of 2 MeV proton beam.

1 Introduction

Determination of a precise impact parameter-dependent interaction potential in the description of ion beam interaction processes in a crystal is important both scientifically and technologically [1, 2]. Axial ion–crystal channeling is a phenomenon that occurs when an ion impinges on a single crystal in a direction close to a major crystallographic axis. A theoretical explanation of channeling was given by Lindhard [3]. This process is explained as a result of the series of correlated small-angle collisions of an ion and atoms of the strings defining the crystal channel [4]. In this transmission, an oscillatory ion motion in space between atomic strings defining the channel is established, i.e., the ion is guided through crystal channels.

The equation of an ion motion through a crystal channel is determined by the interaction potential, which is described by Newton's equations of motion $\mathrm{d}\vec{p}/\mathrm{d}t = -\nabla U_{ch}(\vec{\rho})$, where t is time, $\vec{p}$ is the ion momentum, U_{ch} is the ion–crystal interaction potential, and $\vec{\rho}$ is the transverse vector of ion position relative to the atomic strings defining the crystal channel. Thus, ion channeling can be determined using a precise interaction potential. Frequently used interaction potentials are based on the Thomas–Fermi statistical model of the atom. A good analytical approximation is given by Molière [5]. Another commonly used interaction potential is the Ziegler–Biersack–Littmark (further in text ZBL) one [6]. Original Molière's interaction potential can be applied to the ion–atom scattering process if the influence of the ion on the screening function can be neglected. However, Molière's approximation of the Thomas–Fermi model of an atom can be applied to the ion–atom scattering problem with the use of the screening function proposed by Firsov, which includes the effect of both the ion and the atom [7].

The dominant process that appears in channeling is the crystal rainbow effect, whose theory was formulated by Petrović et al. [8]. This theory accurately predicts the spatial and angular distributions of ions channeled through crystals. The crystal rainbow effect was experimentally confirmed in a series of high-resolution ion transmission channeling experiments through ultra-thin silicon membranes [9]. After that, it was shown that this experimental results and crystal rainbow theory could be used for the determination of a precise rainbow ion–crystal interaction potential [10]. This theory was also used for the explanation of the so-called doughnut effect, which occurs when the ion beam is tilted away from a major crystallographic direction [11]. Recently, it has been shown that the crystal rainbow effect could be used to determine the thermal vibrations and defects of graphene sheets [12, 13]. In this article, we used the crystal rainbow effect to study the channeling of protons through 28 cubic crystals oriented along

Guest editors: Bratislav Obradović, Jovan Cvetić, Dragana Ilić, Vladimir Srećković and Sylwia Ptasinska.

T.I.: Physics of Ionized Gases and Spectroscopy of Isolated Complex Systems: Fundamentals and Applications.

[a] e-mail: nikolas@vin.bg.ac.rs (corresponding author)

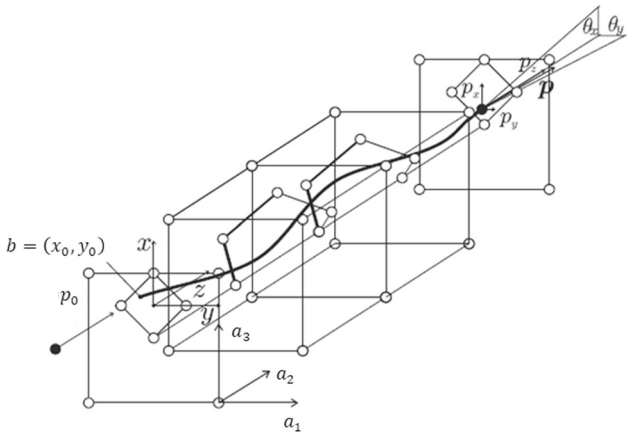

Fig. 1 Scheme of the ion channeling process through square crystal channel

principal crystallographic axes relative to the proton beam.

2 Theory

The scheme of ion channeling through the square channels of cubic crystals is shown in Fig. 1. The z-axis of the reference system is longitudinal and coincides with the axis of the crystal channel, while x and y are vertical and horizontal axes, respectively. In this case, the ion initial impact parameter is given by $b = b(x_0, y_0)$.

The ion–crystal interaction assumes the continuum approximation and the ion–atom binary collision model [4]. In this case interaction potential between the channeled ion and an atomic string defining crystal channel is given as:

$$U_i(x, y) = \frac{1}{d} \int_{-\infty}^{+\infty} V\left[\left(\rho_i^2 + z^2\right)\right]^{1/2} dz, \tag{1}$$

where U_i is the continuum interaction potential of ion and *ith* atomic string, d is the distance between neighboring atoms of atomic string, $\rho_i = \left[(x - x_i)^2 + (y - y_i)^2\right]^{1/2}$ is the distance between ion and *ith* atomic string, x_i and y_i are coordinates of *ith* atomic string, and V is ion–atom interaction potential. Using above-defined ion-string continuum interaction potential we defined ion–crystal continuum interaction potential U_{ch} as the sum of the continuum potentials of all atomic strings forming the channel. The thermal vibrations of crystal atoms were taken into account [8].

The crystal rainbow effect is a consequence of the scattering of ions with differential impact parameters into the same scattering angle. The theory of the crystal rainbows is based on the analysis of mapping of the impact parameter (IP) plane to the transmission angle (TA) plane, determined by the ion scattering/channeling process [8]. As a result of the approximation of the continuum string model, only motion in the transversal plane is taken into account:

$$\theta_x = \theta_x(x_0, y_0) \text{ and } \theta_y = \theta_y(x_0, y_0), \tag{2}$$

where θ_x and θ_y are components of the final ion channeling angle, i.e., components of its transmission angle. This mapping also depends on the ion energy, crystal channel, and thickness, which are all treated as fixed parameters. In order to obtain mapping defined by functions (2), one has to solve ion equations of motion and determine the ion final/exit angle. Initial components of ion positions are selected uniformly in the entrance plane of the crystal, while the initial ion velocity vector v is parallel to the z-axis. The channeled ion scattering angle is smaller than the critical angle for channeling [3, 4], so the components θ_x and θ_y of scattering angles are $\theta_x = v_x/v$ and $\theta_y = v_y/v$, respectively, where v_x and v_y are transverse components of the final ion velocity.

Since the components of the ion channeling angle remain small during the whole transmission process, the ion differential transmission cross section reads [8]:

$$\sigma(x_0, y_0) = \frac{1}{|J_\theta(x_0, y_0)|}, \tag{3}$$

where $J_\theta(x_0, y_0) = \partial_{x_0}\theta_x \partial_{y_0}\theta_y - \partial_{y_0}\theta_x \partial_{x_0}\theta_y$ is Jacobian of the mapping (3). Therefore, the equation:

$$J_\theta(x_0, y_0) = 0 \tag{4}$$

defines the rainbow lines in the impact parameter plane, i.e., the lines in this plane along which $\sigma(x_0, y_0)$ is infinite. The images of the mapping of these lines determined by function (4) are the rainbow lines in the TA plane. Rainbow lines in TA plane separate bright and dark regions. Generally speaking, the rainbow effect represents singularities of the corresponding mappings from the IP plane to the SA plane, meaning that the differential cross section is singular along the rainbow lines. Therefore, the rainbow effect is an example of a singularity effect. We apply the effect of the crystal rainbow in order to construct an accurate rainbow interaction potential via the morphological method comparing the rainbow lines in the TA plane corresponding to the rainbow interaction potential with the rainbow lines in TA plane corresponding to Molière and ZBL interaction potentials.

3 Results

We have analyzed the channeling of 2 MeV protons through 28 crystals with a cubic crystallographic structure in (001) and (111) orientations, i.e., ion channeling through square and triangle crystal channels, respectively. Crystals with the FCC crystallographic structure are: aluminum (Al^{13}), calcium (Ca^{20}), nickel (Ni^{28}), copper (Cu^{29}), strontium (Sr^{38}), rhodium (Rh^{45}), palladium (Pd^{46}), silver (Ag^{47}), cerium (Ce^{58}), ytterbium

(Yb^{70}), iridium (Ir^{77}), platinum (Pt^{78}), gold (Au^{79}), lead (Pb^{82}) and thorium (Th^{90}); with BCC crystallographic structure: vanadium (V^{23}), chromium (Cr^{24}), iron (Fe^{26}), niobium (Nb^{41}), molybdenum (Mo^{42}), barium (Ba^{56}), europium (Eu^{63}), tantalum (Ta^{73}) and tungsten (W^{74}); and crystals with diamond-type crystallographic structure are: carbon (C^{6}), silicon (Si^{14}), germanium (Ge^{32}) and tin (Sn^{50}). Our goal was to construct a universal rainbow channeling interaction potential for all these crystals using the crystal rainbow morphological method [10]. The rainbow lines generated with the rainbow interaction potential were compared with the rainbow lines obtained with Molière and ZBL interaction potentials.

The most frequently used interaction potential for ion–atom scattering is ZBL [6]:

$$V_{\mathrm{ZBL}} = \frac{Z_1 Z_2 e^2}{R} \sum_{i=1}^{4} \alpha_i exp\left(-\frac{\beta_i R}{a_{\mathrm{ZBL}}}\right), \tag{5}$$

where Z_1 is the atomic number of channeled ion, Z_2 is the atomic number of crystal atom, e is the elementary charge, R is the ion–atom distance (the potential is rotationally symmetric), $a_{\mathrm{ZBL}} = \left(9\pi^2/128\right)^{1/3}\left(Z_1^p + Z_2^p\right)^{-1} a_0$ is the ZBL screening radius, a_0 is the Bohr radius,$\alpha_i = (0.1818, 0.5099, 0.2802, 0.2817)$, $\beta_i = (3.2, 0.9423, 0.4028, 0.2016)$ and $p = 0.23$ are the fitting parameters. This potential was obtained by performing an averaging fit of the results of Thomas–Fermi quantum mechanical potential calculated by a Hartree–Fock method. The V_{ZBL} potential was dominantly applied in the scattering process for small ion–atom impact parameters. Even though it was proven accurate for many ion–atom pairs, this interaction potential could not reproduce well high-resolution proton-silicon transmission channeling experiments [10].

On the other hand, in the analysis of their ion channeling experiments through thin Si^{14} crystals, Kraus et al. [14] noticed that angular distributions of channeled ions were better reproduced by using the Molière's approximation of the Thomas–Fermi ion–atom interaction potential, with the Thomas–Fermi atomic screening length. This result was not surprising since the obtained angular distribution of channeled ions was generated by ions that were channeled near the channel axis, i.e., far from the atomic arrays that define the crystal channel.

Molière's ion–atom interaction potential [5] is given by:

$$V_M = \frac{Z_1 Z_2 e^2}{R} \sum_{i=1}^{3} \gamma_i exp\left(-\frac{\delta_i R}{a_{\mathrm{TF}}}\right), \tag{6}$$

where $\gamma_i = (0.1, 0.55, 0.35)$, and $\delta_i = (6, 1.2, 0.3)$ are the fitting parameters, $a_{\mathrm{TF}} = \left(9\pi^2/128\right)^{1/3} Z_2^{-1/3} a_0$ is the atomic Thomas–Fermi screening radius. Molière's interaction potential is justified if the influence of an ion on the screening function can be neglected. However, Molière's interaction potential with Firsov screening radius $a_F = \left(9\pi^2/128\right)^{1/3}\left(Z_1^{1/2} + Z_2^{1/2}\right)^{-2/3} a_0$ instead of a_{TF} can be used, considering ion influence on the screening function [7]. If this is the case, Molière's interaction potential reads, $V_M = \frac{Z_1 Z_2 e^2}{R} \sum_{i=1}^{3} \gamma_i exp\left(-\frac{\delta_i' R}{a_F}\right) = \frac{Z_1 Z_2 e^2}{R} \sum_{i=1}^{3} \gamma_i exp\left(-\frac{\delta_i R}{a_{\mathrm{TF}}}\right)$, where one has to change fitting parameters δ_i to $\delta_i' = (a_F/a_{tf})\delta_i$, where $(a_F/a_{\mathrm{TF}}) = \left(Z_1^{1/2} + Z_2^{1/2}\right)^{-2/3}/Z_2^{-1/3}$ depends on the atomic numbers of both the ion and the crystal Z_1 and Z_2, respectively.

Petrovic et al. [10] successfully described the high-resolution experimental angular distribution of channeled protons with energies of 0.7 to 2 MeV through thin silicon membranes with a thickness of 55 nm, in the (001) orientation, by using the crystal rainbow theory. Modification of the Molière's interaction potential, including the Firsov screening radius, i.e., by changing only the fitting parameter $\delta_2' = 1.025$ to $\delta_2'^{r} = 1.828$, the authors achieved an excellent agreement between the high-resolution experimental angular distributions and the calculated angular distributions, thereby, constructing a rainbow interaction potential that excellently reproduces the experimental angular distribution in the entire channel area. We used the same methodology to construct the universal rainbow interaction potential for different proton-crystal pairs in (001) orientation [15]. Our goal is to, by changing only the fitting parameter δ_2', construct the universal rainbow interaction potential. This universal rainbow interaction potential shall generate an outer rainbow line which very well approximates the outer rainbow line generated with V_{ZBL} and simultaneously will generate an inner rainbow line which also very well approximates the inner rainbow line generated with V_M. It is important to emphasize that the outer rainbow line corresponds to small impact parameters and the inner rainbow line corresponds to large impact parameters.

According to the results presented in Ref. [10] and [16], the fitting parameters $\delta_1'^{r}$ and $\delta_3'^{r}$ are equal to $\delta_i'^{r} = \left[\left(Z_1 + Z_2^{1/2}\right)/Z_2^{1/2}\right]^{2/3} \delta_i'$ $(i = 1, 3)$, while parameter $\delta_2'^{r}$ was adjusted for each crystal. The method for adjusting the parameter $\delta_2'^{r}$ consists of the minimization of the expressions R_{100} for the (001) orientation, and R_{111} for the (111) orientation, which are both equal to $(1/2)\left(\sqrt{((\theta_{xr1} - \theta_{xZBL1})/\theta_{xr1})^2 + ((\theta_{xr2} - \theta_{xM2})/\theta_{xr2})^2}\right)100\%$. Values of R_{100} and R_{111} are the relative distances between the corresponding rainbow lines. By introducing these relative distances, we treated both inner and outer rainbow lines in the same (relative) way. In the (001) orientation, θ_{xr1} and θ_{xr2} are the characteristic rainbow points for large and small angles in TA plane, respectively, that are compared to the

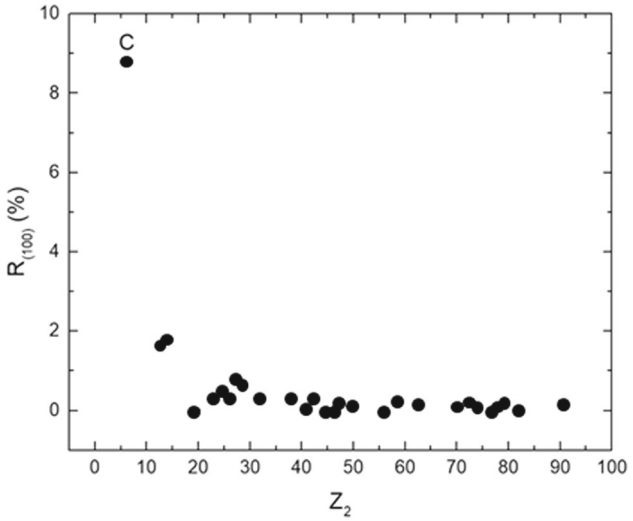

Fig. 2 Calculated values of the relative distances between the rainbow lines for the cubic crystals in the (001) orientation, with distinctively higher values for carbon

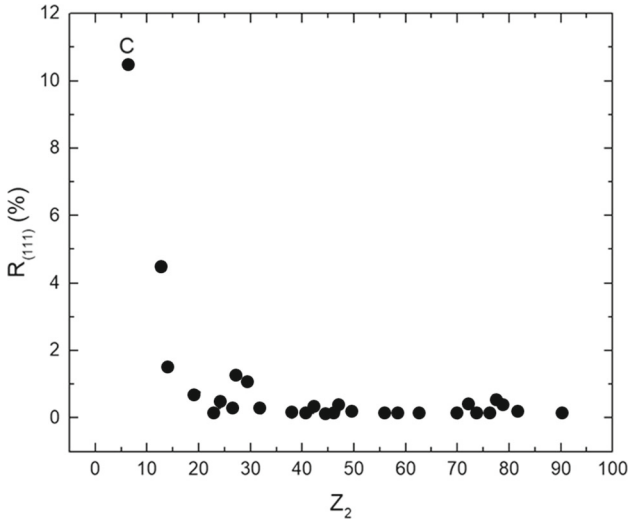

Fig. 3 Calculated values of the relative distances between the rainbow lines for the cubic crystals in the (111) orientation, with distinctively higher values for carbon

corresponding characteristic points θ_{xZBL1} and θ_{xM2} to the points mentioned above lying on the $\theta_x = 0$ axe. Similarly, in the (111) orientation, θ_{xr1} and θ_{xr2} are the characteristic rainbow points for large and small angles in TA plane that are compared to corresponding characteristic points θ_{xZBL1} and θ_{xM2} to the points mentioned above lying on the $\theta_y = 0$ and $\theta_x = 0$ axes, respectively. In the case of 2 MeV protons and the (001) 55 nm thick Si^{14} crystal, this assumption has been experimentally proven [10], and the calculated δ_2^{lr} value for proton-silicon channeling was 1.828, which is very close to the obtained value of $\delta_2^{lr} = 1.85$ for the universal potential (see text below).

Our goal is to obtain a sufficiently separated outer from the inner rainbow lines and to make the outer rainbow line close to the atomic array and the inner rainbow line close to the crystal channel axis. So that the outer rainbow line corresponds to small impact parameters and that, at the same time, the inner rainbow line corresponds to large impact parameters, we adjusted the thickness of all the considered crystals in both orientations. Due to the different channel geometry between these two orientations and the different sizes of channels and atomic crystal numbers, we fixed inner and outer rainbow lines and expressed their positions in the units of the screening radius (SRU).

For all crystals, the calculated parameters R_{100} and R_{111} are small and are presented in Figs. 2 and 3, respectively. The only exception is carbon, for which Coulomb-like ion–atom interaction potential with a screening function cannot be well established because of the small numbers of its electrons. Also, bonds between carbon atoms are strong, resulting in a very small channel, which resulted in the poor separation of inner and outer rainbow lines compared to channel dimensions. Consequently, interaction potentials obtained with another approach, like Doyle-Turner's, would be more appropriate [17]. Also, the R_{111} value for Al^{13} is larger than for other elements but much smaller than for C^6 and remains within the boundaries of acceptable values. Analysis shows that the parameter R_{100} can be set to be less than 3% for the (001) orientation, and the parameter R_{111} can be set to be less than 5% for the (111) orientation. The calculated fitting parameter δ_2^{lr} has the same value for all crystals in the (001) orientation, $\delta_2^{lr} = 1.828$, while this value for the (111) orientation is also the same for all crystals, $\delta_2^{lr} = 1.475$!

Using this morphological methodology, for both crystal orientations, we managed to construct the universal rainbow interaction potential (except for the case of carbon crystals in both crystal orientations). For the (001) orientation constructed the rainbow interaction potential is: $V_{001} = \frac{Z_1 Z_2 e^2}{R} \sum_{i=1}^{3} \gamma_i exp\left(\frac{\delta_i^{lr} R}{a_F}\right)$, where $\gamma_i = (0.10, 0.55, 0.35)$ and $\delta_i^{lr} = \left(Z_2^{1/3}\left(Z_1^{1/2} + Z_2^{1/2}\right)^{-2/3} 6.0, 1.828, Z_2^{1/3}\left(Z_1^{1/2} + Z_2^{1/2}\right)^{-2/3} 0.3\right)$ are the fitting parameters; and for the (111) orientation: $V_{111} = \frac{Z_1 Z_2 e^2}{R} \sum_{i=1}^{3} \gamma_i exp\left(\frac{\delta_i^{lr} R}{a_F}\right)$, where $\delta_i^{lr} = \left(Z_2^{1/3}\left(Z_1^{1/2} + Z_2^{1/2}\right)^{-2/3} 6.0, 1.475, Z_2^{1/3}\left(Z_1^{1/2} + Z_2^{1/2}\right)^{-2/3} 0.3\right)$ is the fitting parameter and $a_F = \left(\frac{9\pi^2}{128}\right)^{1/3}\left(Z_1^{1/2} + Z_2^{1/2}\right)^{-2/3}$ is the Firsov's screening radius.

Figure 4 shows the rainbow lines in the TA plane for ZBL interaction potential, Molière's potential, and the rainbow interaction potentials for the Au^{79} crystal in the (001) orientation. The thickness of the Au^{79} crystal was 27 nm, giving for the 2 MeV protons, well-separated inner and outer rainbow lines close to the channel axis

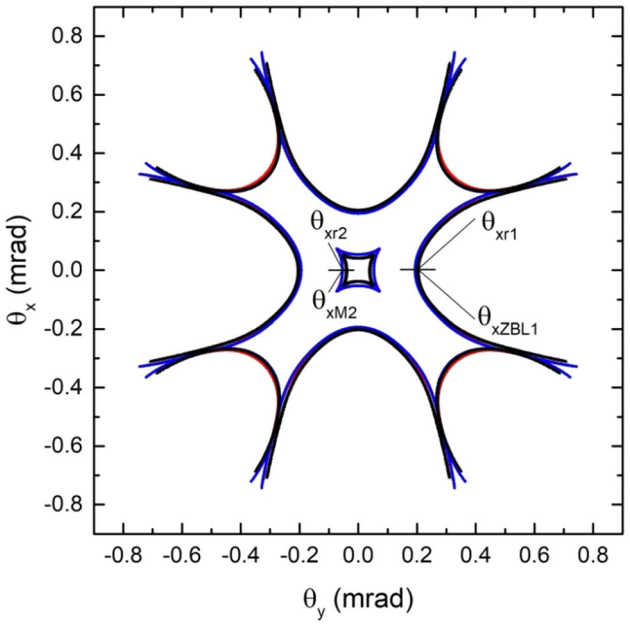

Fig. 4 Rainbow lines in scattering angle plane for 2 MeV protons channeled through 27 nm thin Au^{79} crystal in the (001) orientation; red line—the rainbow interaction potential, blue line—Molière's interaction potential, and black line—ZBL interaction potential

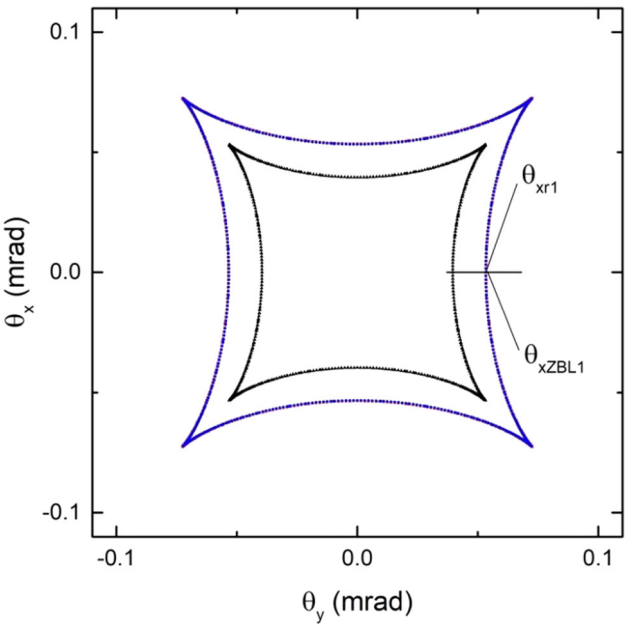

Fig. 5 Larger view of the inner part of the rainbow pattern presented in Fig. 4

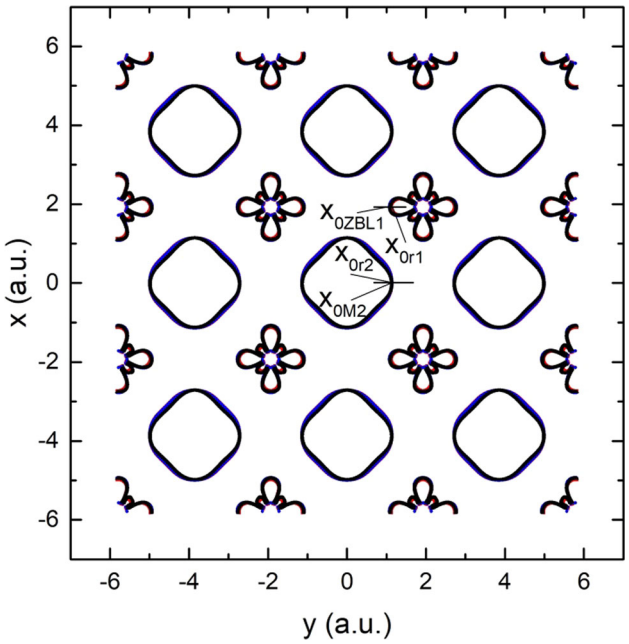

Fig. 6 Rainbow lines in the impact parameter plane for 2 MeV protons channeled through 27 nm thin Au^{79} crystal in the (001) orientation; red line—the rainbow interaction potential, blue line—Molière's interaction potential, and black line—ZBL interaction potential

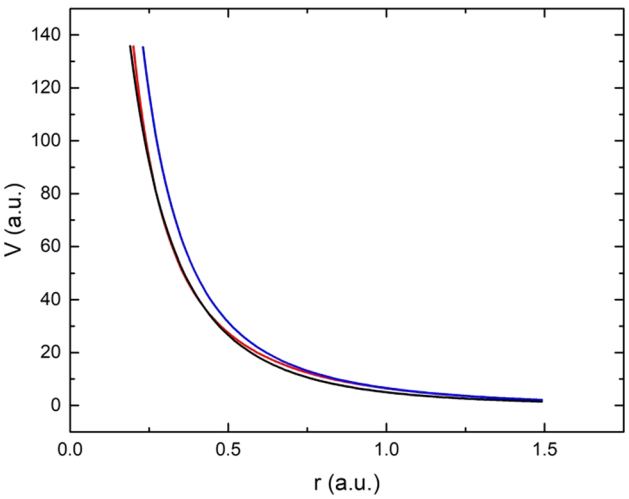

Fig. 7 Dependence of interaction potential on impact parameter for (001) Au^{79} crystal and 2 MeV protons; ZBL interaction potential—black line, Molière's interaction potential—blue line, and the rainbow interaction potentials—red line

and atomic string, respectively. Figure 5 shows a larger view of the inner part of the rainbow pattern presented in Fig. 4.

Figure 6 shows images of rainbow lines in the IP plane. It is clear that the matching between the outer rainbow lines for ZBL, the inner rainbow lines for Molière's potential, and the corresponding rainbow lines generated with the rainbow interaction potential is very well. The choice to present gold crystal was to point out the universality of our morphological approach being accurate for a large atomic number.

Figure 7 shows the dependence of interaction potential on the ion–atom impact parameter for ZBL interaction potential, Molière's potential, and the rainbow

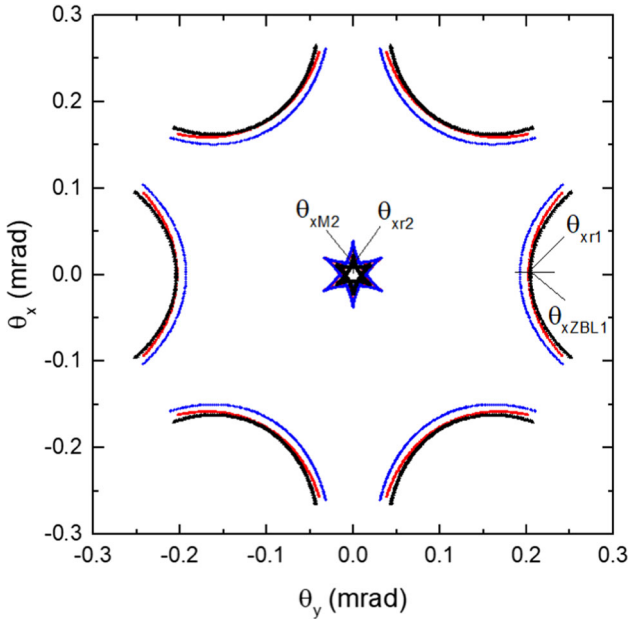

Fig. 8 Rainbow lines in the scattering angle plane for 2 MeV protons channeled through 43 nm thin Si^{14} crystal in (111) orientation; red line—the rainbow interaction potential, blue line—Molière's interaction potential, and black line—ZBL interaction potential

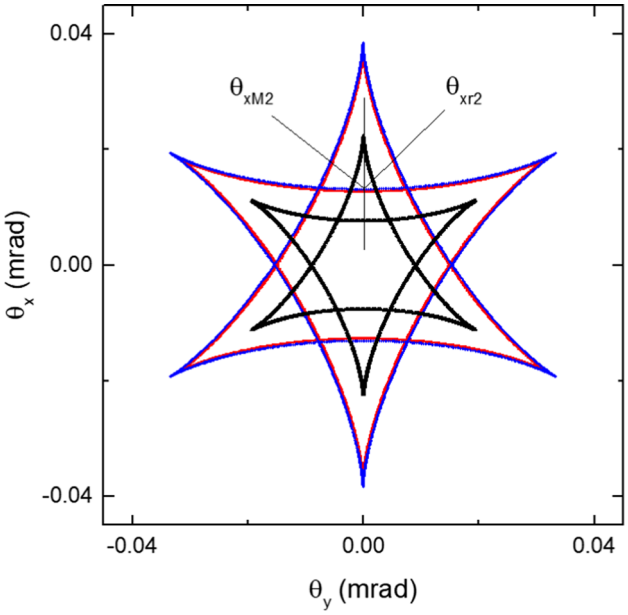

Fig. 9 Larger view of the inner part of the rainbow pattern presented in Fig. 8

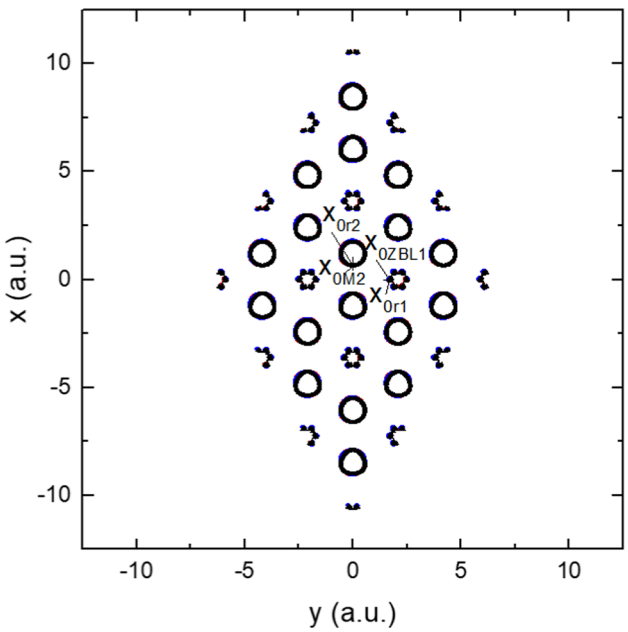

Fig. 10 Rainbow lines in the impact parameter plane for 2 MeV protons channeled through 43 nm thin Si^{14} crystal in the (111) orientation; red line—rainbow interaction potential, blue line—Molière's interaction potential, and black line—ZBL interaction potential

interaction potentials for Au^{79} crystal in the (001) orientation. The constructed rainbow interaction potential is an excellent approximation of Molière's interaction potential for large impact parameters and, at the same time, an excellent approximation of ZBL interaction potential for small impact parameters. Therefore the rainbow potential "glues" both potentials!

Figure 8 shows the same rainbow lines as Fig. 4 but in the case of 43 nm thin (111) Si^{14} crystal. Figure 9 shows a larger view of the inner part of the rainbow pattern presented in Fig. 8. We chose to present the silicon case as an example of the (111) orientation since it has already been experimentally and theoretically proven that our morphological method was the correct one for 55 nm thin (001) Si^{14} crystal [10]. From Fig. 8, the matching of the outer rainbow line generated with the ZBL interaction potential with the outer rainbow line generated with the rainbow interaction potential is very well. At the same time, the matching of the inner rainbow line generated with the Moliere's interaction potential with the inner rainbow line generated with the rainbow interaction potential is also very well. Generally speaking, it should be noted here that the matching of the corresponding rainbow lines could be improved by choosing some other characteristic point on the rainbow lines or trying to globally match the corresponding rainbow lines.

Figure 10 shows images of rainbow lines in the IP plane in the case of 43 nm thin (111) Si^{14} crystal. As well as in the case of above presented 27 nm thin (001) Au^{79} crystal, matching between the corresponding inner and outer rainbow lines is very well.

The rainbow, Molière's, and ZBL interaction potentials dependence on the impact parameter for the (111) silicon crystal case is shown in Fig. 11. It clearly shows and justifies our approach based on the rainbow morphological method for obtaining an accurate rainbow potential. The rainbow potential matches the

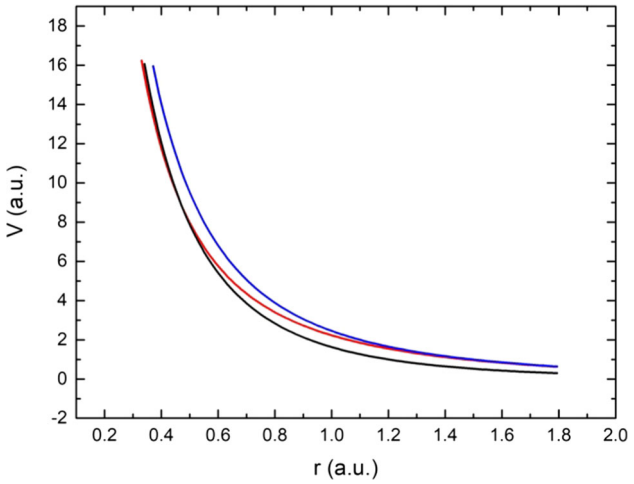

Fig. 11 Dependence of interaction potential on the impact parameter for (111) Si^{14} crystal and 2 MeV protons; ZBL interaction potential—black line, Molière's interaction potential—blue line, and the rainbow interaction potentials—red line

ZBL potential for the small impact parameters and the Molière's potential for the large ones.

As has already been mentioned, carbon crystal is an exception. For the (001) orientation parameter R_{001} has a much bigger value than all other considered crystals, $R_{001} \approx 9\%$. Also, for the (111) orientation value of the parameter is $R_{111} \approx 11\%$. Further, for carbon crystal in both orientations, by changing only the parameter δ_2', it is not possible to make the inner rainbow line generated by the rainbow potential to be close to the inner rainbow line generated by Molière's potential, which is why our morphological method is not suitable for carbon case.

4 Conclusion

In this article, the morphological method for comparing the angular distribution of channeled ions through square and triangle channels of cubic crystals in (001) and (111) orientations, respectively, was employed. It has been shown that the crystal rainbow effect occurs in the angular distributions of channeled ions [8]. We have utilized this effect to construct the universal rainbow ion–atom interaction potential. For both crystal orientations, we managed to construct the universal rainbow interaction potential (except for the carbon case in both orientations).

The obtained fitting parameter δ_2'' for both orientations has different values, namely 1.828 for the (001) orientation and 1.475 for the (111) orientation. We justified this result with the fact that the shape of the channel in these two orientations is different, which is why it is impossible to set identical criteria for small and large impact parameters. Also, we would like to emphasize the lack of angular experimental channeling results for different ion-very thin crystal pairs in transmission mode [10].

Acknowledgements The author acknowledges the support of the Ministry of Science, Technological Development and Innovation of Serbia under the contract No. 451-03-47/2023-01/ 200017.

Author contributions

All authors contributed to the study's conception and design. Material preparation, data collection, and analysis were performed by NS and SP. The first draft of the manuscript was written by NS, and all authors commented on previous versions of the manuscript. All authors read and approved the final manuscript.

Data Availability Statement This manuscript has no associated data or the data will not be deposited. [Authors' comment: The datasets generated during and/or analyzed during the current study are available from the corresponding author upon reasonable request]".

Declarations

Conflict of Interest The authors declare that they have no known competing financial interests or personal relationships that could have appeared to influence the work reported in this paper.

References

1. M. Nastasi, J.W. Mayer, J.K. Hirvonen, *Ion-Solid Interaction: Fundamentals and Applications* (Cambridge University Press, Cambridge, 1996)
2. B. Schmidt, K. Wetzig, *Ion Beams in Materials Processing and Analysis* (Springer, Vienna, 2013)
3. J. Lindhard, Influence of crystal lattice on motion of energetic charged particles. K. Dan. Vidensk. Selsk. Mat.-Fys. Medd. **34**(14), 1–64 (1965). https://doi.org/10.4236/epe.2020.121001
4. D.S. Gemmell, Channeling and related effects in the motion of charged particles through crystals. Rev. Mod. Phys. **46**, 129 (1974). https://doi.org/10.1103/RevModPhys.46.129
5. Gert Moliere, Theorie der Streuung schneller geladener Teilchen I. Einzelstreuung am abgeschirmten Coulomb-Feld. Zeitschrift für Naturforschung A **2**(3), 133–145 (1947). https://doi.org/10.1515/zna-1947-0302
6. J.F. Ziegler, J.P. Biersack, M.D. Ziegler, J.F. Ziegler, J.P. Biersack, U. Littmark, *The Stopping and Range of Ions in Solids* (Pergamon Press, New York, 1985)
7. O.B. Firsov, Calculation of the interaction potential of atoms. Sov. Phys. JETP **6**, 534 (1958)
8. S. Petrović, L. Miletić, N. Nešković, Theory of rainbows in thin crystals: The explanation of ion channeling applied to Ne^{10+} ions transmitted through a <100> Si

thin crystal. Phys. Rev. B **61**, 184 (2000). https://doi.org/10.1103/PhysRevB.61.184
9. M. Motapothula, Z.Y. Dang, T. Venkatesan, M.B.H. Breese, M.A. Rana, A. Osman, Axial ion channeling patterns from ultra-thin silicon membranes. Nucl. Instrum. Methods Phys. Res. B **283**, 29 (2012). https://doi.org/10.1016/j.nimb.2012.04.006
10. S. Petrović, N. Nešković, M. Ćosić, M. Motapothula, M.B.H. Breese, Proton–silicon interaction potential extracted from high-resolution measurements of crystal rainbows. Nucl. Instrum. Methods Phys. Res. B **360**, 23 (2015). https://doi.org/10.1016/j.nimb.2015.07.104
11. M. Motapothula, S. Petrović, N. Nešković, Z.Y. Dang, M.B.H. Breese, M.A. Rana, A. Osman, Origin of ring-like angular distributions observed in rainbow channeling in ultrathin crystals. Phy. Rev. B **86**, 205426 (2012). https://doi.org/10.1103/PhysRevB.86.205426
12. M. Ćosić, M. Hadžijojić, R. Rymzhanov, S. Petrović, S. Bellucci, Investigation of the graphene thermal motion by rainbow scattering. Carbon **145**, 161 (2019). https://doi.org/10.1016/j.carbon.2019.01.020
13. M. Hadžijojić, M. Ćosić, R. Rymzhanov, Morphological analysis of the rainbow patterns created by point defects of graphene. J. Phys. Chem. C **125**, 21030 (2021). https://doi.org/10.1021/acs.jpcc.1c05971
14. H.F. Krause, J.H. Barrett, S. Datz, P.F. Dittner, N.L. Jones, J. Gomez del Campo, C.R. Vane, Angular distribution of ions axially channeled in a very thin crystal: experimental and theoretical results. Phys. Rev. A **49**, 283 (1994). https://doi.org/10.1103/physreva.49.283
15. S. Petrović, N. Starčević, M. Ćosić, Universal axial (0 0 1) rainbow channeling interaction potential. Nucl. Instrum. Meth. Phys. Res. B **447**, 79 (2019). https://doi.org/10.1016/j.nimb.2019.03.050
16. N. Starčević, S. Petrović, Crystal rainbow channeling potential for (001) and (111) cubic crystallographic crystals. Nucl. Inst. Methods Phys. Res. B. **499**, 39 (2021). https://doi.org/10.1016/j.nimb.2021.03.004
17. X. Artru, S.P. Fomin, N.F. Shulga, K.A. Ispirian, N.K. Zhevago, Carbon nanotubes and fullerites in high-energy and X-ray physics. Phys. Rep. **412**, 89 (2005). https://doi.org/10.1016/j.physrep.2005.02.002